Resonant phenomena in compact and extended systems

Kieran Mullen
*Physics Department, Indiana University, Bloomington, Indiana 47405**
and Physics Department, University of Illinois, Urbana, Illinois 61801

Daniel Loss
*IBM T. J. Watson Research Center, Yorktown Heights, New York 10598**
and Physics Department, University of Illinois, Urbana, Illinois 61801

H. T. C. Stoof
*Department of Theoretical Physics, Eindhoven University of Technology, P. O. Box 513, 5600 MB Eindhoven, The Netherlands**
and Physics Department, University of Illinois, Urbana, Illinois 61801
(Received 15 July 1992)

We consider the dynamics of Josephson junctions in two formulations: one where the phase is defined on a compact interval $[0,2\pi]$, and a second where it is defined on an extended interval $(-\infty,\infty)$. We find that in general the two approaches are not equivalent: they have different sets of allowable initial conditions, and similar initial conditions can produce different values for observables. However, they do have identical predictions for the appearance of resonances. These resonances can be understood in a framework of "resonant Zener tunneling," which encompasses resonant tunneling in superlattices, tunneling between Wannier-Stark states in crystals, and Landau-Zener transitions in small metal rings. This framework also reveals a type of resonance in some quantum systems that are strongly driven (i.e., in the sudden limit), wherein the system has a large amplitude to transfer out of the diabatic state.

I. INTRODUCTION

Boundary conditions play a central role in the physics of many mesoscopic systems. For example, persistent currents in normal metal rings can be viewed as arising from the single-valued boundary condition imposed on the electronic wave function on a small ring.[1–6] Or, in narrow wires, a key insight in the Landauer-Büttiker approach is to move all dissipative effects out of the system and embed them in the boundary conditions.[7–9] Often a proper understanding of the boundary conditions is crucial to understanding how one passes from the quantum to the classical limit in such mesoscopic systems.[10]

In this paper we consider some unusual features of yet another system, the Josephson junction. Josephson junctions have proven to be a rich source of physics since the prediction of the Josephson effect.[11] Traditionally they have been studied using the washboard potential [Fig. 1(a)] so that they are described by the Schrödinger equation:

$$i\hbar\frac{\partial\psi}{\partial t}=-\frac{2e^2}{C}\frac{\partial^2\psi}{\partial\theta^2}+\left[\frac{\hbar I}{2e}\theta+E_J(1-\cos\theta)\right]\psi\ , \quad (1)$$

where e is the elementary electronic charge, C is the capacitance of the junction, I is the classical (c number) current, E_J is the Josephson coupling energy, and θ is the phase difference across the junction. We are not interested here in the effect of dissipation, which is commonly represented by terms proportional to $\dot{\theta}$. In this formulation the phase θ is considered to be defined on the extended interval, $\theta\in(-\infty,\infty)$. In particular, the limit that the pair-charging energy $E_C\equiv 2e^2/C$ is much smaller than the Josephson coupling energy, has been studied extensively.[12–16]

More recently, with the advent of microfabrication technologies, it has become possible to work in a regime where the charging energy dominates the coupling energy, so that $E_C>E_J$. Unusual effects have been predicted[17–20] and some have been observed in experiments.[21–24] When considering this limit, Eq. (1) is often rewritten as

$$i\hbar\frac{\partial\varphi}{\partial t}=\frac{2e^2}{C}\left[-i\frac{\partial}{\partial\theta}-\frac{I}{2e}t\right]^2\varphi+E_J(1-\cos\theta)\varphi\ . \quad (2)$$

In this formulation the current is coupled to the operator $\hat{n}\equiv -i\partial/\partial\theta$ instead of the phase. The charge operator $\hat{n}$ represents the number of pairs transferred across the junction. This simple change motivated consideration of coherent charging effects in normal metal junctions, where the phase θ is not well defined.[17] Note that Eq. (2) can be obtained from Eq. (1) by means of a time-dependent gauge transformation:

$$\varphi(\theta,t)=\psi(\theta,t)e^{iI\theta t/2e}\ . \quad (3)$$

Equation (2) has the advantage that it is invariant under the transformation $\theta\rightarrow\theta+2\pi$; obviously Eq. (1) is not. It has been claimed that since the wave functions $\varphi(\theta,t)$ and $\psi(\theta,t)$ are related by a gauge transformation, the physics of the two problems must be identical.[25] This is simply not the case; when making such a change one must also gauge transform the *boundary conditions.* If we

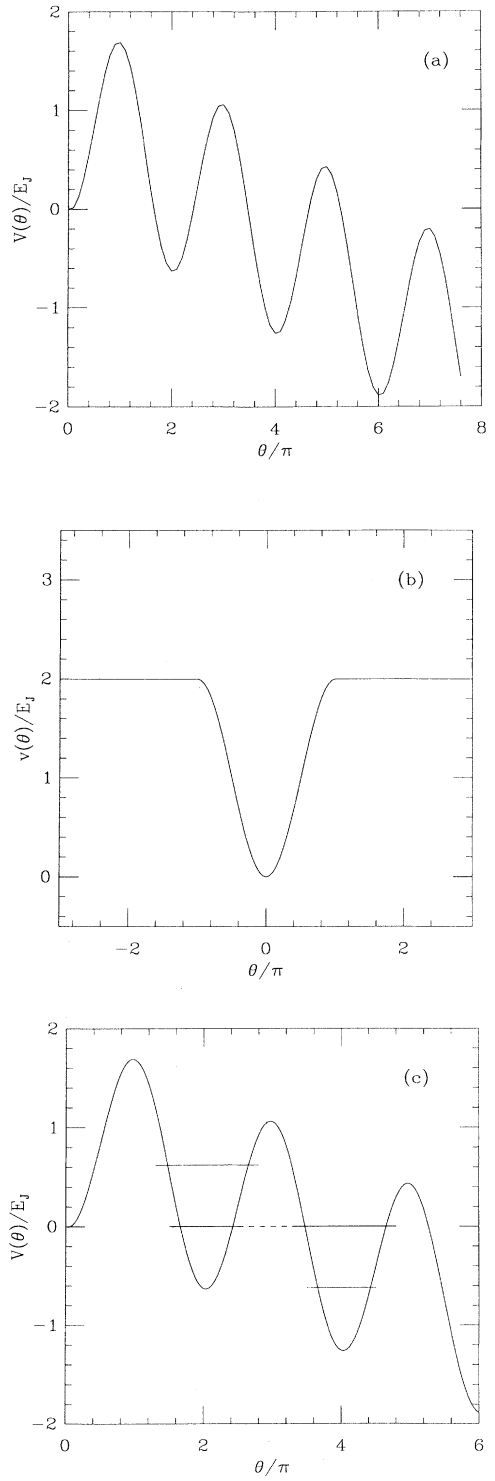

FIG. 1. (a) A schematic representation of the washboard potential; it extends infinitely in both directions. Here it is drawn with a "tilt" or driving force $I/I_J=0.10$. (b) A single well of the washboard potential, embedded in a constant background potential. The eigenstates of this system correspond to unbound resonances in the full washboard potential. (c) A schematic representation of resonant tunneling in the washboard potential. At the appropriate tilt (or external current), states in different wells have the same energy, allowing elastic tunneling.

start out with periodic boundary conditions for φ,

$$\varphi(\theta,t)=\varphi(\theta+2\pi,t)\ , \tag{4}$$

then upon transformation we obtain the time-dependent boundary conditions

$$\psi(\theta,t)=\psi(\theta+2\pi,t)e^{i2\pi It/2e}\ . \tag{5}$$

These time-dependent boundary conditions are never used for solving the washboard Hamiltonian of Eq. (1). In fact, the boundary condition on ψ is often not clearly stated.

The notion that θ should be compact and periodic, with wave functions periodic on the interval $[0,2\pi]$, as opposed to extended, with wave functions defined on the interval $(-\infty,\infty)$, has caused some discussion in the literature.[17,25,26,28–30] In particular there has been some question whether dissipation renders the distinction moot.[26,27,29] Since the effect of dissipation is as yet unresolved, it is sensible to ask if there is any physical difference between the two approaches. It is not *a priori* clear that there must be a difference, since all observables are periodic in θ. If there is none, then questions involving dissipation are irrelevant.

Furthermore, it has recently been suggested that one can observe resonant tunneling phenomena in a *single* Josephson junction.[31,32] If one considers a single period or "well" of the washboard potential at zero bias [Fig. 1(b)], then for the appropriate choice of parameters it is possible to have a finite number of discrete states in the well. While such states are not true eigenstates of the full potential, at low bias currents, ($I \ll I_J \equiv 2eE_J/\hbar$), they will decay only slowly with time. This tunneling rate can be enhanced if the bias current is adjusted such that the energy of one quasibound state of one well aligns with that of a neighbor [Fig. 1(c)]. Such resonant tunneling phenomena are common in superlattices where the bias is an external electric field. In a junction, the resonance would be observed by enhanced transition rates from [Fig. 1(c)] the zero-voltage state to the running state.[32] However, if θ is only defined on the interval $(0,2\pi)$, then it is not *a priori* clear that there is a second well into which the system may resonantly tunnel. Understanding the effect of the boundary conditions is essential to understanding this question.

In this paper we address the role of boundary conditions on the time-dependent Schrödinger equation given in Eq. (2). Specifically, we are interested in the question of whether we obtain fundamentally different physical results if we work on a compact, periodic interval, or on an infinite, extended one. In Sec. II we show numerically and analytically that the two cases are *not* identical. We show that the set of allowable initial conditions is different for the two cases. In addition, there exist interference terms in the compact case that are not present in the extended case. We conclude the section by comparing numerical solutions of the time-dependent Schrödinger equation for the extended and compact problems, demonstrating that the two produce different values for observables.

In Sec. III we examine whether or not resonances

found in the extended description are present in the compact formulation of the problem. We find numerically that the resonances do indeed exist, and that they are present at the same value of the bias current. We show analytically that such resonances are due to a hidden symmetry of the time-dependent Schrödinger equation, a symmetry that allows for resonant Zener tunneling or an enhanced transition rate out of the ground state at a particular value of the driving force. To investigate this issue in detail, we consider a simple two-state time-dependent system and show how such resonance develop. In particular, we show that resonance is not only an adiabatic phenomenon, but can be observed in the sudden limit as an "antiresonance," or a tendency to *not* follow the diabatic states in systems in which the driving force is large.

In Sec. IV we conclude with a general discussion of how the formalism applies to other mesoscopic systems, and the possible effects of dissipation.

II. DIFFERENCES BETWEEN THE COMPACT AND EXTENDED DESCRIPTIONS

In this section we will demonstrate that the compact and extended descriptions of the Josephson junction are not equivalent. In order to do so we will reformulate the problem so that the difference in boundary conditions is rewritten as a difference in initial conditions. We will then show that the domains of initial conditions of the two problems are not identical, and that there are dynamic interference terms present in the compact case that are not present in the extended case.

We must decide at the outset what constitutes a meaningful difference between the compact and extended approaches. For example, the uncertainty of the phase ($\langle \Delta\theta^2 \rangle$) can assuredly differ in extended and compact problems. Moreover, in periodic systems the phase itself is not an observable, and $\langle \Delta\theta^2 \rangle$ is not defined.[33,34] (However, commutators of the form $[\hat{\theta},\hat{n}]$ can be evaluated, as shown in Ref. 34.) We will restrict ourselves to considering operators involving $\sin\hat{\theta}, \cos\hat{\theta}$, and $\hat{n}$, which can all be related to observables, and are invariant under $\theta \rightarrow \theta + 2\pi$. Our goal is to determine if there is a difference between the expectation value of any of these quantities in the extended and compact cases.

We further note that we are not concerned with determining the effect of boundary conditions on the extended case itself; we presume that there is little difference if we choose either the wave function to go to zero as $\theta \rightarrow \pm\infty$, or Born-von Karman boundary conditions. In fact, we will see shortly that it is convenience to solve the extended problem on a large ring. We therefore chose to work with Eq. (2) for both the compact and periodic cases. This avoids the problem of dealing with the unbounded linear potential present in Eq. (1), as well as peculiar problems in satisfying the boundary conditions at infinity.[35]

Having settled on the form of the time-dependent Schrödinger equation, it is convenient to rewrite Eq. (2) in dimensionless form. If we introduce the parameters $\lambda \equiv E_J/E_C$ nd $\beta \equiv \hbar I/2eE_c = \lambda I/I_J$, as well as the dimensionless time variable $s = It/2e$, then we obtain

$$i\beta\frac{\partial}{\partial s}\varphi(\theta,s) = \left[\left[-i\frac{\partial}{\partial\theta} - s\right]^2 + \lambda(1-\cos\theta)\right]\varphi(\theta,s) \ . \quad (6)$$

The time s is related to the number of Cooper pairs that the current source has brought to the junction. We shall use this form of the Schrödinger equation for both the compact and extended cases. At all times we will use the symbol φ for wave functions on the compact interval, and ψ for wave functions on the extended interval, with subscripts where appropriate.

In order to put the extended and compact cases on a more equal footing, we consider our system to be a ring of radius N, let ζ be the polar angle, and let θ be the arc length around the circle, so that $\theta \in (0, 2\pi N)$, as shown in Fig. 2. There are therefore N periods of our cosine potential, and in the limit $N \rightarrow \infty$ we expect to recover the results for the infinite extended interval. We can denote this system together with its periodic boundary conditions by $\mathcal{E}$, and solutions on $\mathcal{E}$ by $\psi(\theta,s)$, with a distinguishing subscript when necessary. When studying the problem numerically for finite N, we must consider only times that are short compared to the time it takes a wave packet to spread around the ring.

We can make a connection to solutions of the compact problem in the following manner. Let $\mathcal{C}$ be the compact, periodic interval $[0,2\pi]$, and $\varphi(\theta,s)$ be a solution of Eq. (6) on $\mathcal{C}$ with initial condition $\varphi_0(\theta)$. We can take $\varphi(\theta,s)$ on $\mathcal{C}$ and use it to create a solution $\psi_c(\theta,s)$ on $\mathcal{E}$, a solution that leads to expectation values of periodic observables which are indistinguishable from those obtained from $\varphi(\theta,s)$ on $\mathcal{C}$. We do this simply by starting with an initial condition on $\mathcal{E}$ that is a periodic repetition of the initial condition $\varphi_0(\theta)$, with the appropriate normalization, as shown in Fig. 3.

It is intuitively clear that if we reproduce $\varphi_0(\theta)$ every 2π on $\mathcal{E}$, the result is the same as solving the original compact problem on $\mathcal{C}$; any effect that the wave function in one well has on its neighbor to the right is exactly equal to the effect on the wave function by its neighbor from the left. We can show this rigorously by taking Fourier transforms. We express $\varphi(\theta,s)$,the solution of Eq. (6) on $\mathcal{C}$, as

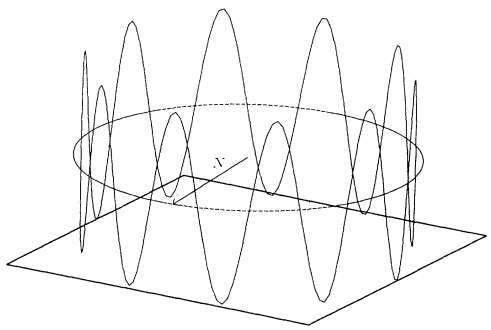

FIG. 2. A picture of the extended periodic potential used in solving Eq. (6) on $\mathcal{E}$, plotted with a radius $N=10$. In all analytic work one must take $N \rightarrow \infty$ at the end of the calculation. In numerical work, N must be sufficiently large so that it does not affect the result.

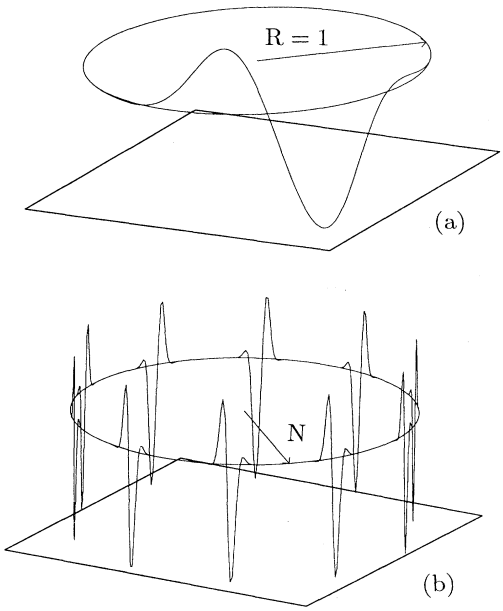

FIG. 3. (a) An initial condition for a compact problem on $\mathcal{C}$, where $\theta\in(0,2\pi)$. (b) The periodic extension of that initial condition onto $\mathcal{E}$. With the appropriate scaling, the value of any observable calculated in the compact interval will be the same as that calculated on the extended interval when the initial conditions are extended periodically.

$$\varphi(\theta,s)=\sum_{k=-\infty}^{\infty} a_k(s)e^{ik\theta}\ , \tag{7}$$

where k is an integer. We can obtain a difference-differential equation for the $a_k(s)$ from Eq. (6).

$$i\beta\dot{a}_k(s)=(k-s)^2a_k(s) -(\lambda/2)[a_{k+1}(s)+a_{k-1}(s)-2a_k(s)]\ . \tag{8}$$

We now assume that the $a_k(s)$ for the solution $\varphi(\theta,s)$ of Eq. (8) are known.

If we follow the same procedure on $\mathcal{E}$, we can expand any general $\psi(\theta,s)$ by

$$\psi(\theta,s)=\sum_{m=-\infty}^{\infty} b_m(s)e^{im\theta/N}\ , \tag{9}$$

and substitute this into Eq. (6) to obtain a similar result:

$$i\beta\dot{b}_m(s)=(m/N-s)^2b_m(s) -(\lambda/2)[b_{m+N}(s)+b_{m-N}(s)-2b_m(s)]\ . \tag{10}$$

We now wish to consider the specific case where $\psi(\theta,s)=\psi_c(\theta,s)$, the periodic repetition of $\varphi(\theta,s)$ on $\mathcal{E}$.[36] To find $\psi(\theta,s)_c$ we simply multiply Eq. (7) by the normalization factor $1/\sqrt{N}$, and allow θ to run from 0 to $2\pi N$. That is, we set

$$b_m(s)=\begin{cases}\dfrac{a_k(s)}{\sqrt{N}} & \text{for } m=kN\\ 0 & \text{otherwise}\ .\end{cases} \tag{11}$$

If the $a_k(s)$ satisfies Eq. (8), then the $b_k(s)$ given in Eq. (11) will satisfy Eq. (10), so that $\psi_c(\theta,s)$ is a solution of the time-dependent Schrödinger equation on $\mathcal{E}$. This holds because the difference equation couples only amplitudes with $\delta k=\pm1$, or equivalently, $\delta m=\pm N$.

If $\hat{A}$ is some operator, then we may calculate its expectation value in the state $|\psi_c(s)\rangle$.

$$\begin{aligned}\langle\psi_c(s)|\hat{A}|\psi_c(s)\rangle&=\int_0^{2\pi N}d\theta\,\psi_c^*(\theta,s)A(\theta)\psi_c(\theta,s)\ ,\\ &=\frac{1}{N}\sum_k\sum_{k'}\int_0^{2\pi N}d\theta\,a_k(s)^*a_{k'}(s)e^{-ik\theta}A(\theta)e^{ik'\theta}\ ,\\ &=\sum_k\sum_{k'}a_k(s)^*a_{k'}(s)\int_0^{2\pi}d\theta\,e^{-ik\theta}A(\theta)e^{ik'\theta}\ ,\end{aligned} \tag{12}$$

where $A(\theta)$ is $\hat{A}$ in the θ representation, so that $A(\theta)\equiv\langle\theta|\hat{A}|\theta\rangle$. Here we have used the fact that $A(\theta)$ can only depend on $\sin\theta$, $\cos\theta$, and $n=-i\partial/\partial\theta$. We see that if we periodically extend the initial condition of a compact problem and solve it on $\mathcal{E}$, we obtain the same values for observables as if we had solved the problem on $\mathcal{C}$.

We are now in a position to see immediately why the compact and extended cases are not equivalent. While any initial condition $\varphi_0(\theta)$ on $\mathcal{C}$ can be translated into an initial condition on $\mathcal{E}$, the converse is not true. An arbitrary initial condition $\psi_0(\theta)$ on $\mathcal{E}$ which is not periodic in 2π cannot be forced onto $\mathcal{C}$ without producing different results. Any Fourier components in $\psi_0(\theta)$ for noninteger m/N cannot be represented on $\mathcal{C}$. Since the extended problem admits solutions which cannot be present in the compact case, the two are different.

There exists a deeper difference between the two cases. To demonstrate this, we will show that if we start with the same initial conditions for the two models, we get different results. In order to do so, we must first define what we mean by the "same initial conditions."

Above we have discussed how to take an initial condition $\varphi_0(\theta)$ on $\mathcal{C}$ and develop an equivalent initial condition on the extended system $\mathcal{E}$ that reproduces all of the physics of the compact case We wish to compare this with the result we would get if we had started out solving the problem on $\mathcal{E}$ originally. That is, we wish to find

$\psi_e(\theta,s)$, the solution on the extended system $\mathcal{E}$, with the initial condition

$$\psi_e(\theta,0)=\begin{cases}\varphi_0(\theta) & \text{for } 0<\theta<2\pi\ , \\ 0 & \text{for } 2\pi<\theta<2\pi N\ .\end{cases} \tag{13}$$

This is what we mean by the "same initial conditions" for the two models. The motivation for this definition is that an initial condition for the extended approach is most often a wave packet localized in a single well.

The advantage of this formulation of the problem is that we are now dealing with solutions to the *same* Hamiltonian with the *same* boundary conditions, $[\psi(\theta+2\pi N,s)=\psi(\theta,s)]$, and have reduced the difference to the initial conditions. Once we have $\psi_e(\theta,s)$ and $\psi_c(\theta,s)$, we can compare the expectation value of some operator $\hat{A}$ for the two approaches:

$$\langle \hat{A} \rangle_{e(s)}=\langle \psi_e(s)|\hat{A}|\psi_e(s)\rangle\ ,$$
$$\langle \hat{A} \rangle_{c(s)}=\langle \varphi(s)|\hat{A}|\varphi(s)\rangle$$
$$=\langle \psi_c(s)|\hat{A}|\psi_c(s)\rangle\ . \tag{14}$$

Our goal is thus to find out if there is any difference between $\langle \hat{A} \rangle_{e(s)}$ and $\langle \hat{A} \rangle_{c(s)}$.

Assume that we know the solution to the extended problem, $\psi_e(\theta,s)$, where the initial condition is as given in Eq. (13), so that it is nonzero only in the first well. Since $\psi_c(\theta,0)$ is a periodic repetition of $\psi_e(\theta,0)$, with each copy offset by a multiple of 2π, the time evolution of $\psi_c(\theta,s)$ is just a superposition of copies of $\psi_e(\theta,s)$, with the same offsets. That is

$$\psi_c(\theta,s)=\frac{1}{\sqrt{N}}\sum_{j=0}^{N-1}\psi_e(\theta-2\pi j,s)\ . \tag{15}$$

Inserting this into our expressions for $\langle \hat{A} \rangle_{c(s)}$,

$$\begin{aligned}\langle \hat{A} \rangle_{c(s)}&=\langle \psi_c(s)^*|\hat{A}|\psi_c(s)\rangle \\ &=\frac{1}{N}\sum_{j=0}^{N-1}\sum_{j'=0}^{N-1}\int_0^{2\pi N}d\theta\,\psi_e(\theta-2\pi j,s)^*A(\theta)\psi_e(\theta-2\pi j',s) \\ &=\sum_{l=0}^{N-1}\int_0^{2\pi N}d\theta\,\psi_e(\theta-2\pi l,s)A(\theta)\psi_e(\theta,s)\ ,\end{aligned} \tag{16}$$

where we have used the periodicity of $\mathcal{E}$. The difference between the extended and compact results is

$$\langle \hat{A} \rangle_{c(s)}-\langle \hat{A} \rangle_{e(s)}=\sum_{l=1}^{N-1}\langle \psi_e(\theta-2\pi l,s)|\hat{A}|\psi_e(\theta,s)\rangle\ . \tag{17}$$

We see from Eq. (17) that the difference between the two models arises from interference (overlap) terms between amplitudes that start in different wells. In the extended problem, in the limit $N\to\infty$, the spreading wave function does not interfere with itself; in the compact problem, the wave function cannot spread without "meeting itself" in the next well.

In general, the interference term of Eq. (17) is not zero. Moreover, its dependence upon the parameter λ is unusual. In the limit that $\lambda\to\infty$, interference will be absent since tunneling is suppressed and the different wells decouple. In the opposite limit, $\lambda\to 0$, it is possible to calculate the interference contribution exactly, as shown in the Appendix. There we find that any difference in the voltage will be time independent; other observables such as the current need not be. The difference in calculated observables conclusively shows that the compact and extended formulations are not equivalent. In order to see a dynamic difference in the voltage and voltage fluctuations between the two models we need consider $\lambda\gtrsim 1$.

To calculate the general difference in observables given in Eq. (17), we must solve Eq. (6) for arbitrary λ. Unfortunately this is analytically intractable. To see why this is so, we will try to find the instantaneous eigenstates of Eq. (6) on $\mathcal{C}$. treating s as a time-independent parameter, we must solve the equation

$$\left[\left[-i\frac{\partial}{\partial\theta}-s\right]^2+\lambda(1-\cos\theta)\right]\varphi(\theta,s)=E(s)\varphi(\theta,s)\ . \tag{18}$$

This may be put into standard form by means of the substitutions $y(\theta,s)=\varphi(\theta,s)e^{is\theta}$, $q=\lambda/2$, $a=\lambda-E$, and $z=\theta/2$ to obtain

$$y''(z,s)+(a-2q\cos 2z)y(z,s)=0 \tag{19}$$

subject to the boundary condition $y(z+\pi,s)=y(z,s)e^{i2\pi s}$. This is the general form of the Mathieu equation.[37]. When s is not an integer, then the solutions are Mathieu function of fractional order $\delta=s-[s]$. There are no closed form expressions for these functions for arbitrary δ and λ, so it is not possible to make the standard adiabatic approximation for $\varphi(\theta,s)$ by expanding in terms of the instantaneous eigenstates.

We shall therefore attack the problem numerically. The eigenvalue problem is well suited to a power-method approach. The eigenvalues of Eq. (18) were calculated using a power method, and are plotted in Fig. 4 for various values of λ. Such an energy-band structure is common to a variety of systems, including electrons moving in a lattice, and a small normal metal ring driven by an external flux. The periodicity of the bands will be discussed in detail below.

The time-dependent Schrödinger equation can be solved using the implicit method.[38] We solve Eq. (6) on $\mathcal{E}$ using the initial conditions given in Eqs. (13) and (15).

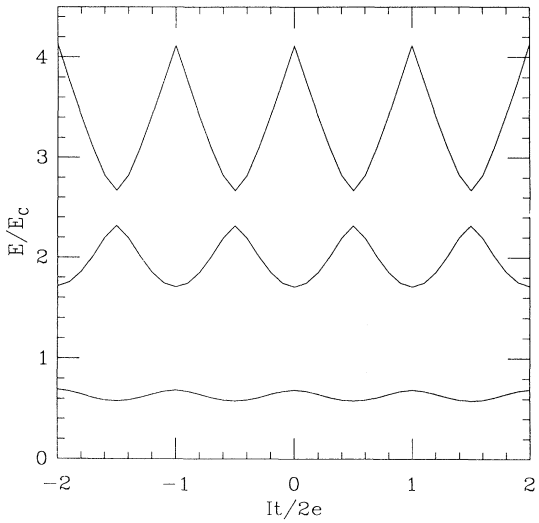

FIG. 4. The three lowest bands of the energy spectrum of Eq. (18), for $\lambda = E_J/E_C = 1.0$. Note that the gaps close rapidly with increasing band number; the rate-limiting step is Zener tunneling out of the lowest band.

For fixed N, we can discretize our interval into small steps, and calculate the time evolution of $\psi(\theta,s)$. The results must be checked to be independent of N, the discretization mesh, and the time step.

We calculate $\langle \hat{n} \rangle$, the expectation value of the difference in the number of Cooper pairs on each side of the junction, which is proportional to the voltage across the device; and $\langle \hat{n}^2 \rangle$, which can be related to the voltage fluctuations. Typical results are plotted in Fig. 5. We see that $\langle \hat{n}^2 \rangle_{(s)}$ starts off the same, but soon becomes different for the two models. As a check, we know *a priori* that $\langle \hat{n} \rangle_{(s)}$ should be zero for our choice of a symmetric initial condition. We find that $\langle \hat{n} \rangle^2 / \langle \hat{n}^2 \rangle < 10^{-12}$, indicating that the solutions are numerically accurate. The fact that $\langle \hat{n}^2 \rangle$ is not the same for the two models demonstrates numerically that the compact and extended versions of the problem are *not* equivalent.

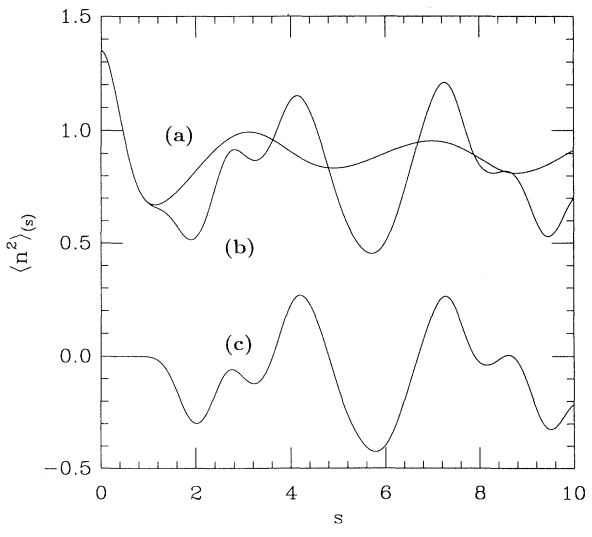

FIG. 5. Numerical $\langle \hat{n}^2 \rangle$ for the extended and compact cases. Line (a) is for the extended case, line (b) is for the compact case, and line (c) is the difference of the two. The parameters are $\lambda = 1.0$ and $\beta = 0.0$. The initial condition was the ground state of the compact problem for $\lambda = 16.0$.

In this section we have seen that the extended formulation of the problem admits certain initial conditions not found in the compact case, and there are dynamical interference terms present in time evolution of the compact case which are not found in the extended problem. It is apparent that the two approaches are not equivalent. Any calculation of Josephson junction dynamics, analytical or numerical, should take this into account.

III. RESONANCES IN DRIVEN QUANTUM SYSTEMS

A. Resonances in current-driven Josephson junctions

In Sec. II we have shown that the compact and extended approaches to the phase variable can produce different results for observables. We now consider a more specific physical question: is the resonant tunneling behavior of the extended approach also present in the compact case? For the sake of concreteness, we examine this question in the context of Josephson junctions; the result may be generalized to other systems.

It should be stressed that the resonant tunneling we refer to in Josephson junctions is fundamentally different from resonant tunneling in multiple quantum well structures. In the quantum well case, we apply an external electric field to an electron in a potential $V_0(x)$ of period a_0:

$$H_{qw} = -\frac{\hbar^2}{2m}\frac{\partial^2}{\partial x^2} - eEx + V_0(x) \ . \tag{20}$$

If $\Delta\epsilon$ is the splitting between the lowest two states of a single well, then the condition for the resonance, or elastic tunneling, from one well to another is

$$\Delta\epsilon = eEa_0 \ . \tag{21}$$

That is, for an electric field of strength $E = \Delta\epsilon/ea_0$, the ground state of one well will line up with the excited state of the adjacent well. Clearly in this case the spatial coordinate x is an extended variable.

In the Josephson case there is only a single junction; the resonant tunneling in the extended approach is not from one spatial location to another. Rather, the relevant variable is the phase difference of the superconducting wave function across the junction. Changes in this collective coordinate represent many changes in the microscopic coordinates of the pairs (and thereby the electrons) that make up the system. The possibility of tunneling in such macroscopic variables, even in the presence of dissipation, has been demonstrated by experiments on the switching rates of Josephson devices.[12–16] Such experiments were performed on devices with $\lambda \equiv E_J/E_C \gg 1$. In the case of resonant tunneling, how-

ever, we are interested in the regime where there are few quantum states in each well. If we approximate the cosine potential as a parabola, and calculate the number of states with energy less than E_J, we can set an upper limit of $\sqrt{\tilde{\lambda}}/2$ quantum states per well.[32] We are therefore interested in $\lambda \gtrsim 1$.

Although the notion of resonant tunneling in an extended phase description seems intuitively reasonable, it carries with it several problems. It is not obvious how to choose an appropriate initial condition: does the system always start with all of its amplitude localized in one well? Thermal averaging over a variety of initial conditions is not possible, as the energy spectrum is unbounded below. It is assumed that a measurement of the supercurrent across the junction would fix the wave function to be in one well, but it is not clear that this is the case.[32] Furthermore, the unbounded nature of the energy causes a variety of problems for calculation of the subsequent dynamics.[35]

In order to determine the presence of the resonant tunneling in the compact description we solve Eq. (8) numerically. This number representation is superior to the phase representation of Eq. (6) because in the latter, the wave function becomes highly oscillatory in θ as time increases, with frequency components $k \propto s$. Solving this in the θ representation would require an exceedingly fine discretization.

To obtain an initial condition we solve the time-independent Schrödinger equation (setting $\beta=0$) for the ground-state wave function, with some particular value of the coupling $\tilde{\lambda}$. We then evolve this wave function forward in time (perhaps with a different value of the coupling) and evaluate the expectation value of the voltage at some particular time s_0,

$$\langle V \rangle_{(s_0)} = (2e/C)\langle \varphi(s_0)|\hat{n}|\varphi(s_0)\rangle \ . \tag{22}$$

For $\lambda \ll 1$, here is only one bound state in the single well potential plotted in Fig. 1(b) and there is no possibility for resonant tunneling. For $\lambda \gg 1$, the tunneling rate is too small for practical experiments because the tunneling barrier is too large. In Fig. 6 we show the results of the numerical calculations for intermediate values of λ. We see the clear presence of a resonance near $\beta \approx 0.30$, since there is an enhanced probability for the system to make a transition out of the lowest band and thus increase the average voltage. This resonance is at the same value as predicted by the extended approach. At larger values of the current ($\beta \lesssim 1$), the junction is always in the running state and the voltage increases linearly in time.

The quantum-mechanical transition from one band to another due to an external driving force is known as Zener tunneling.[39–44] Here we seen an enhanced rate of resonance for the transition at a particular value of the driving force. In considering the dynamics of transitions among the bands, the existence of enhanced or resonant Zener tunneling has not been previously recognized.

We are thus presented with a puzzle: what is the source of such resonant behavior in the compact system, which does not have the "tilted well" structure? The answer lies in examining the structure of Eq. (6). We

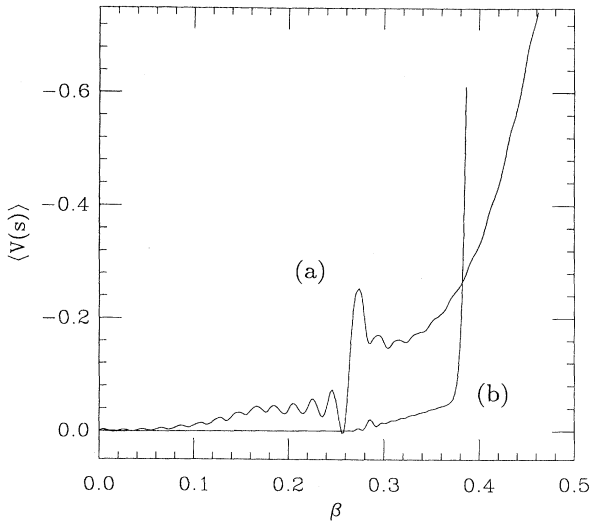

FIG. 6. Demonstration of resonances in the compact case. The expectation value of the voltage is plotted at $s = It/2e = 50$ for different values of the applied current, β. The parameters are $\lambda = 4.0$ (a) and $\lambda = 8.0$ (b); the initial condition was taken to be the ground state with $\beta = 0$. The abrupt, monotonic change in the voltage on the right-hand side of the graph is due to depinning. The oscillatory structure signals the presence of resonant tunneling, or enhanced transition rates between the bands.

note that there is a symmetry hidden in the time-dependent Schrödinger equation; if we let $s \rightarrow s+1$ in the Hamiltonian, and $\varphi \rightarrow e^{i\theta}\varphi$, we recover the original equation. This symmetry is made manifest in the periodic structure of the energy bands of Fig. 4. In Sec. III B below, we will show that by properly exploiting this symmetry, we can obtain the resonance observed in Fig. 6, using the compact description. We will apply this first to a simple two-level system in Sec. III C, and then in Sec. III D, the Josephson junction problem.

B. Resonances in periodically driven two-level systems

In the compact description of the Josephson junction we have an energy spectrum with an infinite number of bands (Fig. 4). Since the key element is the periodicity of the system in time, rather than the details of the energy spectrum, we may examine a problem with a finite number of bands. We will consider the simplest case, with just two bands. Our goal is to determine if, for some value of the parameters, there is a marked increase in the transition rate from one band to another. We will refer to such behavior as a resonance, or resonant Zener tunneling.

Consider a two-level system driven by an external force, so that the adiabatic energy spectrum is periodic as a function of time, with just two bands. If we start with the system in a state $|\Psi(0)\rangle$, then after a time t, we will be in the state $|\Psi(t)\rangle$ given by

$$|\Psi(t)\rangle = \hat{U}(t)|\Psi(0)\rangle \ , \tag{23}$$

where $\hat{U}(t)$ is the time-evolution operator. If τ_0 is the fundamental period of the energy spectrum, then from $\hat{U}(\tau_0)\equiv\hat{U}_0$ we can find the state of the system at a time $t=n\tau_0$ by taking powers of $\hat{U}_0$:

$$|\Psi(n\tau_0)\rangle=(\hat{U}_0)^n|\Psi(0)\rangle \ . \tag{24}$$

If we work in a matrix representation, then the time evolution operator $\hat{U}_0$ is simply viewed as a transfer matrix relating the final and initial states as the system goes through a single period. We wish to establish what features of U_0 determine that there is a resonance. We can then relate these features to physical parameters of a concrete problem.

The time evolution operator is unitary, so its most general form in a 2×2 matrix representation is

$$U_0=e^{i\delta}\begin{bmatrix} e^{i\alpha}\cos\phi & e^{i\gamma}\sin\phi \\ -e^{-i\gamma}\sin\phi & e^{-i\alpha}\cos\phi \end{bmatrix} , \tag{25}$$

where the Zener tunneling probability in one period is $\sin^2\phi$. If we know the eigenvalues and eigenvectors of U_0 in some basis, then we may follow the time evolution of some arbitrary state $|\Psi(\tau)\rangle$ [represented as a spinor $\Psi(\tau)$ in the same basis], at multiples of the fundamental period. We simply need to expand $\Psi(0)$ in terms of the eigenvectors, $\mathbf{e}_\pm$, of U_0, with eigenvalues $\mu_\pm$:

$$\Psi(0)=a_+\mathbf{e}_+ + a_-\mathbf{e}_- \ , \tag{26}$$

and use Eq. (24) to obtain the final result

$$\begin{aligned}\Psi(n\tau_0)&=(U_0)^n\Psi(0)\\ &=(U_0)^n(a_+\mathbf{e}_+ + a_-\mathbf{e}_-)\\ &=a_+\mu_+^n\mathbf{e}_+ + a_-\mu_-^n\mathbf{e}_- \ .\end{aligned} \tag{27}$$

Such transfer matrix techniques are more commonly used in one-dimensional statistical mechanics problems.[45]

It is a simple matter to determine the eigenvalues $\mu_\pm$ of this matrix:

$$\mu_\pm=e^{i\delta}(\cos\alpha\cos\phi\pm i\sqrt{1-\cos^2\alpha\cos^2\phi}) \ . \tag{28}$$

Note that because of gauge invariance the eigenvalues are independent of γ but do depend upon α, the relative phase of the diagonal elements. If we introduce the angle η such that $\cos\eta=\cos\alpha\cos\phi$ (so α, η, and ϕ are the sides of a right spherical triangle, with η as the hypotenuse), then

$$\mu_\pm=e^{i(\delta\pm\eta)} \ . \tag{29}$$

The corresponding eigenvectors $\mathbf{e}_\pm$ are

$$\begin{aligned}\mathbf{e}_+&=N\begin{bmatrix} e^{i\gamma}\sin\phi \\ -i(\sin\alpha\cos\phi-\sqrt{1-\cos^2\alpha\cos^2\phi}) \end{bmatrix} ,\\ \mathbf{e}_-&=-N\begin{bmatrix} i(\sin\alpha\cos\phi-\sqrt{1-\cos^2\alpha\cos^2\phi}) \\ e^{i\gamma}\sin\phi \end{bmatrix} ,\end{aligned} \tag{30}$$

with the normalization constant N equal to

$$N=[\sin^2\phi+(\sin\alpha\cos\phi-\sqrt{1-\cos^2\alpha\cos^2\phi})^2]^{-1/2} \ . \tag{31}$$

Let the system start in only one state, say $(0,1)^T$. Then we may expand the initial state in terms of the eigenvectors $\mathbf{e}_\pm$, and calculate the time evolution as in Eq. (27). With a bit of algebra we find that $P_0(n)$, the probability to remain in the initial state after n iterations, is

$$\begin{aligned}P_0(n)&=|\langle\Psi(0)|\Psi(n\tau_0)\rangle|^2\\ &=1+2B[\cos(2n\eta)-1] \ ,\end{aligned} \tag{32}$$

where the amplitude of the oscillation is given by

$$B=\frac{(\sin\alpha\cos\phi+\sqrt{1-\cos^2\alpha\cos^2\phi})^2\sin^2\phi}{[(\sin\alpha\cos\phi+\sqrt{1-\cos^2\alpha\cos^2\phi})^2+\sin^2\phi]^2} \ . \tag{33}$$

The amplitude B determines how much probability is transferred between the two bands. It takes on a maximum value of $\frac{1}{4}$ when

$$\alpha=m\pi \ , \tag{34}$$

for any integer m, and at this value, the probability to be in $|\Psi(0)\rangle$ oscillates from zero to unity and back. Equation (34) is the condition for resonant Zener tunneling. For other values of α the transition rate between the bands is smaller,and the probability to stay in the state $|\Psi(0)\rangle$ never falls to zero.

When the tunneling rate is small so that $\phi\ll1$, the amplitude B is a sharply peaked function of α, with a width of order $\sim\phi$, as is shown in Fig. 7. These are the resonances we seek. If we slowly vary α when $\phi\ll1$, then we see a dramatic increase in the transition rate whenever α is a multiple of π. This occurs because, when the transition rate per period is small, it takes many periods for an amplitude to accumulate in the upper state. Each sub-

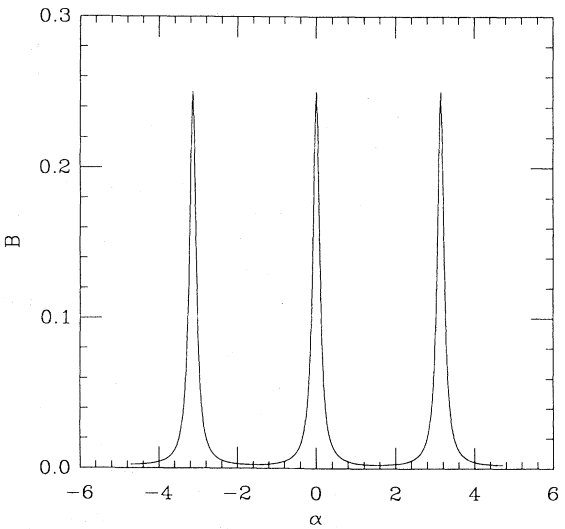

FIG. 7. A plot of B, the amplitude of the oscillations between the bands of a two-level system, as a function of α, the phase difference between the diagonal elements of the transfer matrix. The value of ϕ, which is approximately the tunneling amplitude [Eq. (25)], is 0.1. An exact analytical expression for B is given in Eq. (33).

sequent addition of amplitude at each period can add either in or out of phase with the amplitude transferred in the previous period. If it is added out of phase, it cancels the previous contribution and there is no net oscillation between the levels. If it adds exactly in phase with the previous contribution, there is a large and rapid transfer of amplitude between the levels.

C. Example of resonances in a two-level system

As a specific example of the behavior described above, we consider a spin-$\frac{1}{2}$ particle in a time-dependent magnetic field. We will apply an oscillating magnetic field in the z direction and simultaneously a constant one in the x direction. The Hamiltonian for the system is

$$H_\sigma=\mu_0 B_z \sin\omega t\,\hat{\sigma}_z+\mu_0 B_x\hat{\sigma}_x \ , \tag{35}$$

where $\hat{\sigma}_z$ and $\hat{\sigma}_x$ are Pauli spin matrices. We may reduce this to dimensionless form by scaling the time variable to $\tau=\omega t$, and introducing the parameters $a=\mu_0 B_z/\hbar\omega$ and $b=\mu_0 B_x/\hbar\omega$, so that our time-dependent Schrödinger equation is

$$i\frac{\partial}{\partial\tau}\Psi(\tau)=(a\sin\tau\hat{\sigma}_z+b\hat{\sigma}_x)\Psi(\tau) \ . \tag{36}$$

Without loss of generality, we may restrict a and b to be positive.

In order to implement the analysis of the previous section, we must calculate the matrix elements of the time evolution operator $\hat{U}_0$. Assume that we have two orthogonal states, $|\Psi_1(0)\rangle$ and $|\Psi_2(0)\rangle$, which serve as the initial conditions (at time τ_i), to two time-dependent solutions of Eq. (36), $|\Psi_1(\tau)\rangle$ and $|\Psi_2(\tau)\rangle$, respectively. Then the matrix U_0 is

$$U_0=\begin{bmatrix}\langle\Psi_1(0)|\Psi_1(\tau_f)\rangle & \langle\Psi_2(0)|\Psi_1(\tau_f)\rangle\\ \langle\Psi_1(0)|\Psi_2(\tau_f)\rangle & \langle\Psi_2(0)|\Psi_2(\tau_f)\rangle\end{bmatrix} , \tag{37}$$

where $\tau_f-\tau_i=2\pi$. We must therefore solve Eq. (36) for different initial conditions and calculate these elements. Generally, this cannot be done exactly. We will therefore develop approximate solutions in the adiabatic and sudden limits.

If we work in the $|\hat{\sigma}_z\rangle$ basis and label the components of $\Psi(\tau)$:

$$\Psi(\tau)=\begin{bmatrix}p(\tau)\\ q(\tau)\end{bmatrix} , \tag{38}$$

then Eq. (36) is equivalent to the couple equations

$$\begin{aligned} i\dot{p}(\tau)&=a\sin\tau\,p(\tau)+bq(\tau) \ ,\\ i\dot{q}(\tau)&=-a\sin\tau\,q(\tau)+bp(\tau) \ . \end{aligned} \tag{39}$$

We first examine this problem in the adiabatic limit. We need to solve the auxiliary problem.

$$\begin{aligned} \epsilon(\tau)p(\tau)&=a\sin\tau p(\tau)+bq(\tau) \ ,\\ \epsilon(\tau)q(\tau)&=-a\sin\tau q(\tau)+bp(\tau) \ , \end{aligned} \tag{40}$$

where we treat τ as a parameter, and $\epsilon(\tau)$ is the quasienergy or "instantaneous energy." Writing Eq. (40) as a 2×2 matrix and solving for the determinant, we find

$$\epsilon_\pm(\tau)=\pm\sqrt{a^2\sin^2\tau+b^2} \ , \tag{41}$$

with the instantaneous eigenstates

$$\begin{aligned} \Psi_+(\tau)&=\tilde{N}\begin{bmatrix}-b\\ a\sin\tau-\sqrt{a^2\sin^2\tau+b^2}\end{bmatrix} ,\\ \Psi_-(\tau)k&=\tilde{N}\begin{bmatrix}a\sin\tau-\sqrt{a^2\sin^2\tau+b^2}\\ b\end{bmatrix} , \end{aligned} \tag{42}$$

where $\tilde{N}$ is the normalization constant:

$$\tilde{N}=\frac{1}{\sqrt{2}}[a^2\sin^2\tau+b^2-a\sin\tau\sqrt{a^2\sin^2\tau+b^2}]^{-1/2} \ . \tag{43}$$

The instantaneous energy as a function of τ is plotted in Fig. 8. We choose $\tau_i=\pi/2$ and $\tau_f=5\pi/2$ so that we integrate over a full period of the Hamiltonian, from one point of maximum energy separation to another. Note that the energy spectrum is π periodic, twice that of the Hamiltonian itself. In studying Zener tunneling transitions, it is the structure an symmetry of the Hamiltonian itself, and not simply that of the energy spectrum that is relevant.[41]

We can use these instantaneous eigenstates to construct a solution to Eq. (36). We write

$$\begin{aligned} \Psi(\tau)=&A_+(\tau)\Psi_+(\tau)e^{-i\int^\tau d\tau'\epsilon_+(\tau')}\\ &+A_-(\tau)\Psi_-(\tau)e^{-i\int^\tau d\tau'\epsilon_-(\tau')} \ . \end{aligned} \tag{44}$$

Substituting this expression into Eq. (36) we find, after a little algebra,

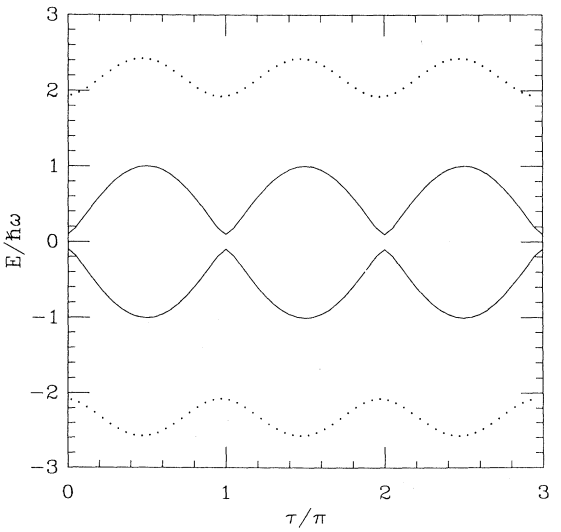

FIG. 8. A plot of the instantaneous energies of Eq. (40) as given in Eq. (41). The solid line is in the sudden limit, with $a=1.0$ and $b=0.10$. The dotted line is in the adiabatic limit, with $a=1.5$ and $b=2.0$. Note that the period of the energy spectrum is half that of the Hamiltonian.

$$[\dot{A}_+(\tau)\Psi_+(\tau)+A_+(\tau)\dot{\Psi}_+(\tau)]e^{-i\int^\tau d\tau'\epsilon_+(\tau')}$$
$$+[\dot{A}_-(\tau)\Psi_-(\tau)+A_-(\tau)\dot{\Psi}_-(\tau)]e^{-i\int^\tau d\tau'\epsilon_-(\tau')}=0\ . \tag{45}$$

Multiplying from the left with $\Psi_+^*(\tau)$ we obtain

$$\dot{A}_+(\tau)=-A_-(\tau)\Psi_+^*(\tau)\dot{\Psi}_-(\tau)e^{i\int^\tau d\tau'[\epsilon_+(\tau')-\epsilon_-(\tau')]}\ , \tag{46}$$

where we note in passing that $\Psi_+^*(\tau)\dot{\Psi}_+(\tau)=0$. A similar equation can be derived for $\dot{A}_-(\tau)$.

Up to this point our calculations have been exact. In order to make progress we assume that the transition amplitudes from one band to another *in one period* $(\tau_f-\tau_i)$ are small. (This is a weak restriction on the parameters; we do not require that the transition rate over several periods be small.) We are interested in enhanced transition rates between the adiabatic states, and therefore choose $|\Psi_+(0)\rangle$ and $|\Psi_-(0)\rangle$ as our basis states for calculating the matrix elements of U_0. To do so, we start with $A_-(0)=1$ and $A_+(0)=0$, and then calculate $A_+(\tau)$ and $A_-(\tau)$ after one period. We then repeat the calculation starting with $A_+(0)=1$ and $A_-(0)=0$, and again calculate $A_+(\tau)$ and $A_-(\tau)$ after one period. Due to the symmetry of U_0, we need only focus on the first of these two calculations.

We first examine the off-diagonal elements that describe the interband transitions. We start with $A_-(0)=1$ and $A_+(0)=0$, and then calculate $A_+(\tau)$ after one period. In the adiabatic approximation we assume that since the rate of transition is small, then $A_-(\tau)\approx 1$, and from Eq. (46) we have

$$A_+(\tau_f)\approx\int_{\tau_i}^{\tau_f}d\tau'\Psi_+^*(\tau')\dot{\Psi}_-(\tau')\times e^{i\int d\tau''[\epsilon_+(\tau'')-\epsilon_-(\tau'')]}$$
$$\equiv\int_{\tau_i}^{\tau_f}d\tau' G(\tau')e^{i\int^{\tau'}d\tau'' F(\tau'')}\ . \tag{47}$$

The exponent $F(\tau')$ is given by

$$F(\tau')=\int^{\tau'}d\tau''[\epsilon_+(\tau'')-\epsilon_-(\tau'')]$$
$$=2\int^{\tau'}d\tau''\sqrt{a^2\sin^2\tau''+b^2}$$
$$=2b\int^{\tau'}d\tau''\sqrt{1+(a/b)^2\sin\tau''}\ , \tag{48}$$

which can be related to an incomplete elliptic integral of the second kind. The exact result is not particularly illuminating. Instead it is more fruitful to approximate $F(\tau')$ for $a/b\ll 1$. We find

$$F(\tau')=2b\sqrt{1+(a/2b)^2}\int^{\tau'}d\tau''\sqrt{1-\rho\cos 2\tau''}$$
$$\approx 2b\sqrt{1+(a/2b)^2}\int^{\tau'}d\tau''[1-\tfrac{1}{2}\rho\cos 2\tau''-\tfrac{1}{8}\rho^2\cos^2 2\tau''+\cdots]\ , \tag{49}$$

where ρ is

$$\rho\equiv\frac{(a/b)^2}{2+a^2/b^2}\ . \tag{50}$$

Performing the integrals in Eq. (49) and grouping terms of equal order we get

$$F(\tau')\approx a\sqrt{2/\rho}\left[\left[1-\frac{\rho^2}{16}\right]\tau'-\frac{\rho}{4}\sin 2\tau'-\frac{\rho^2}{64}\sin 4\tau'+\cdots\right]+\Phi_0\ , \tag{51}$$

where Φ_0 is some constant that affects the overall phase. Expanding the exponential up the terms of order a^2/b we find

$$e^{iF(\tau')}\approx e^{i(\omega_0\tau'+\Phi_0)}\left[J_0\left[\frac{a}{4}\sqrt{2\rho}\right]+iJ_1\left[\frac{a}{4}\sqrt{2\rho}\right]\sin 2\tau'+\cdots\right]\ , \tag{52}$$

where

$$\omega_0\equiv a\sqrt{2/\rho}(1-\rho^2/16)\ , \tag{53}$$

and $J_n(x)$ is the Bessel function of integral order n.

The prefactor $G(\tau)$ can be found using Eq. (42) to produce

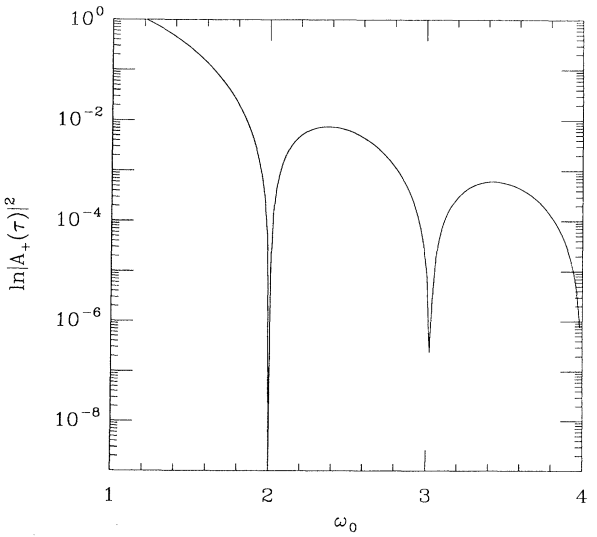

FIG. 9. The log of the transition probability after a single period in the adiabatic limit, plotted as a function of ω_0. The parameters are $a=0.5$ and $b\in(0.5,2.0)$. Numerical solutions of the time-dependent Schrödinger equation [Eq. (39)] and the analytic approximation [Eq. (55)] agree to within the thickness of the lines. At even multiples of ω_0 the transition probability is zero.

$$G(\tau)=\frac{ab}{2}\frac{\cos\tau}{a^2\sin^2\tau+b^2}\ . \tag{54}$$

Upon expansion in powers of ρ, this prefactor will have only odd Fourier components in τ. Putting this together with Eq. (52) into Eq. (46) produces a number of simple exponentials that can be trivially integrated. We introduce $\tilde{\omega}_0\equiv\omega_0+i\nu$, taking $\nu\to 0$ at the end of calculation in order to avoid ambiguities about poles. The leading behavior for the transition amplitude is then

$$\begin{aligned}A_+(\tau_f)\approx\lim_{\nu\to 0}e^{i\phi_0}\frac{b\rho}{a}\Bigg\{&\frac{1}{2}\left[1-\frac{\rho^2}{16}\right]J_0\left[\frac{a}{4}\sqrt{2\rho}\right]\left[\frac{e^{i\pi(\tilde{\omega}_0+1)}}{\tilde{\omega}_0+1}+\frac{e^{i\pi(\tilde{\omega}_0-1)}}{\tilde{\omega}_0-1}\right]\\&+\frac{\rho}{4}J_0\left[\frac{a}{4}\sqrt{2\rho}\right]\left[\frac{e^{i\pi(\tilde{\omega}_0+1)}}{\tilde{\omega}_0+1}+\frac{e^{i\pi(\tilde{\omega}_0-1)}}{\tilde{\omega}_0-1}+\frac{e^{i\pi(\tilde{\omega}_0+3)}}{\tilde{\omega}_0+3}+\frac{e^{i\pi(\tilde{\omega}_0-3)}}{\tilde{\omega}_0-3}\right]\\&+\frac{1}{2}J_1\left[\frac{a}{4}\sqrt{2\rho}\right]\left[\frac{e^{i\pi(\tilde{\omega}_0+1)}}{\tilde{\omega}_0+1}-\frac{e^{i\pi(\tilde{\omega}_0-1)}}{\tilde{\omega}_0-1}+\frac{e^{i\pi(\tilde{\omega}_0+3)}}{\tilde{\omega}_0+3}-\frac{e^{i\pi(\tilde{\omega}_0-3)}}{\tilde{\omega}_0-3}\right]\Bigg\}\Bigg|_{\tau_i}^{\tau_f}\ .\end{aligned} \tag{55}$$

Despite the seeming appearance of singular behavior, a little algebra shows that the expression is finite for integral ω_0 (that is, as $\nu\to 0$). In Fig. 9 we plot $|A_+|^2$ vs ω_0 for a single period. Direct numerical solution of the differential equations in Eq.(39) yields identical results to this expansion to within the width of the plotted lines. Note that the amplitude is zero at even multiples of ω_0. This occurs because $G(\tau)$ contains only odd Fourier components, and is orthogonal to the expansion given in Eq. (52), when ω_0 is an even integer.

We now look at the diagonal elements of the time evolution matrix given in Eq. (37). In the adiabatic limit, if $A_-(\tau_i)=1$, after one period $A_-(\tau_f)$ will be nearly the same. However, the state will have accumulated an overall phase given by the integral of the instantaneous energy over one period, as can be seen from the coefficient of Ψ_- in Eq. (44). according to Eq. (34), a resonance should occur when the accumulated phase *difference* between the diagonal elements of the time evolution matrix is a multiple of π, or

$$\begin{aligned}\alpha&=\frac{1}{2}\int_0^{2\pi}d\tau[\epsilon_+(\tau)-\epsilon_-(\tau)]\\&=\int_0^{2\pi}d\tau\sqrt{a^2\sin^2\tau+b^2}\\&\approx\frac{1}{2}a\sqrt{2/\rho}(1-\rho^2/16)(2\pi)=n\pi\ ,\end{aligned} \tag{56}$$

or more simply

$$\omega_0=n\ , \tag{57}$$

where we have expanded the square root as in Eq. (49) and integrated over a full period, canceling all the trigonometric terms. The final expression gives us a condition on when the energy tunneling resonance should occur. Thus the transfer-matrix approach predicts a maximum in the transition rate between the two bands whenever Eq. (57) is satisfied.

We may solve Eq. (39) numerically, and explicitly determine the matrix elements given in Eq. (37). The numerical solution does not rely on any of the expansions and approximations made to obtain the analytic results of Eqs. (55) and (56). It provides an entirely independent check of the calculations. Numerical solutions in the adiabatic regime for the transition probability after a single period are in excellent agreement with the analytic calculations (Fig. 9); we see that the transition amplitude is zero for $\omega_0=2n$, as predicted. In Fig. 10 we plot numerical solutions of the differential equation of Eq. (39) for an integer number of periods. We observe a strong enhancement in the probability of being in the adiabatic state as a function of ω_0 at odd multiples, as predicted. Note that the resonance is not due to a maximum of the transition probability over a single period; it is only after many periods that this peak develops.

Next we consider the sudden limit, where one expects the system to follow the diabatic states. The same arguments developed above apply here. The resonance now manifests itself as a tendency for the system to *not* follow the diabatic states, and thus *not* follow the driving force. Such a peculiar situation can be called an antiresonance.

In the sudden limit it is no longer appropriate to work in the adiabatic basis states. Instead, we wish to calculate the matrix elements of U_0 in the σ_z basis. Let us denote the basis states

$$\Psi_1=\begin{bmatrix}1\\0\end{bmatrix}\ ,\quad \Psi_2=\begin{bmatrix}0\\1\end{bmatrix}\ , \tag{58}$$

and let $\Psi_1(\tau)$ be the solution of Eq. (40) with $\Psi_1(0)=\Psi_1$. We introduce a new set of functions

$$\begin{aligned}u(\tau)&=p(\tau)e^{ia\cos\tau}\ ,\\v(\tau)&=q(\tau)e^{-ia\cos\tau}\ ,\end{aligned} \tag{59}$$

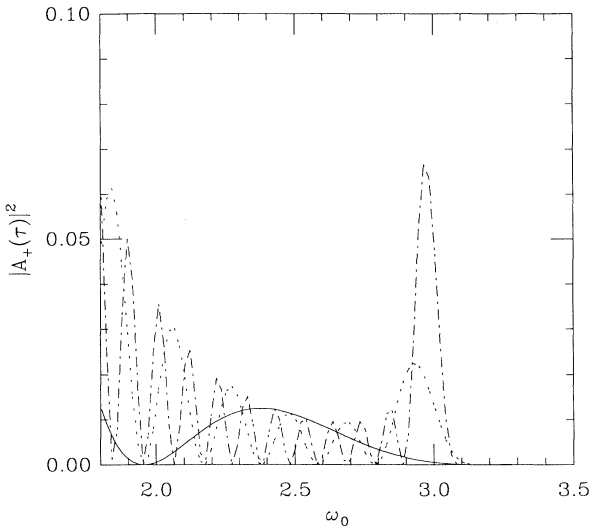

FIG. 10. Plot of resonances in the transition probability as a function of ω_0 in the adiabatic limit. The parameters are $a=0.50$, $b\in(1.0,3.0)$. The sold line is the transition probability after one period; the dashed line is the result after 10 periods; the dash-dot line is the result after 20 periods. The peak appears at $\omega_0=3$ a predicted. Resonances at higher n start with a lower initial transition rate, and must be iterated for more periods in order to see the peak.

which upon substitution into Eq. (39) yield the differential equations

$$i\dot{u}(\tau)=bv(\tau)e^{-2ia\cos\tau}\ ,$$
$$i\dot{v}(\tau)=bu(\tau)e^{2ia\cos\tau}\ . \tag{60}$$

As in the adiabatic case, we wish to solve Eq. (60) with the initial condition $\Psi(0)=\Psi_1$, which is equivalent to starting with $p(0)=u(0)=1$ and $q(0)=v(0)=0$. The sudden limit is obtained when the time rate of change of the driving force is so large that the system tends to stay in the same state. We can get an approximation for the transition amplitude by assuming $u(\tau)$ is constant, and integrating

$$\begin{aligned} v(\tau_0)&\approx -ib\int_0^{2\pi}d\tau\, e^{2ia\cos\tau}\\ &=-ib\int_0^{2\pi}d\tau\sum_{n=-\infty}^{\infty}J_n(2a)e^{in\tau}\\ &=-2\pi ib\,J_0(2a)\ . \end{aligned} \tag{61}$$

Whenever $2\pi bJ_0(2a)\ll 1$ we are in the sudden limit.

According to the understanding developed in Sec. III B, a resonance will occur when the phase difference between the diagonal elements accumulated over the course of a period is a multiple of π as in Eq. (34). The relative phase of the diagonal elements is just $2a\cos\tau$. Integrating this over a single period *always* yields zero, so that the resonance condition is always trivially satisfied. This is shown in Fig. 11 where we calculate the transition rate after several periods, and see that it is simply a multiple of the transition rate after a single period.

In order to see the effect we desire in the sudden limit, we must introduce an additional phase shift between the diagonal elements by means of a small constant magnetic field in the z direction,

$$H'_\sigma=\mu_0(B_z\sin\omega t+B_{0z})\hat{\sigma}_z+\mu_0B_x\hat{\sigma}_x \tag{62}$$

so that our time-dependent Schrödinger equation now becomes

$$i\frac{\partial}{\partial\tau}\Psi(\tau)=[(a\sin\tau+\kappa)\hat{\sigma}_z+b\hat{\sigma}_x]\Psi(\tau)\ , \tag{63}$$

where $\kappa\equiv\mu_0B_{0z}/\hbar\omega$. Again we introduce a new set of functions

$$\begin{aligned} p(\tau)&=\tilde{u}(\tau)e^{-i(a\cos\tau-\kappa\tau)}\ ,\\ q(\tau)&=\tilde{v}(\tau)e^{i(a\cos\tau-\kappa\tau)}\ , \end{aligned} \tag{64}$$

which obey the differential equations

$$\begin{aligned} i\frac{\partial}{\partial\tau}\tilde{u}(\tau)&=b\tilde{v}(\tau)e^{2i(a\cos\tau-\kappa)}\\ i\frac{\partial}{\partial\tau}\tilde{v}(\tau)&=b\tilde{u}(\tau)e^{-2i(a\cos\tau-\kappa)}\ . \end{aligned} \tag{65}$$

Performing a similar expansion to that of Eq. (61) we obtain

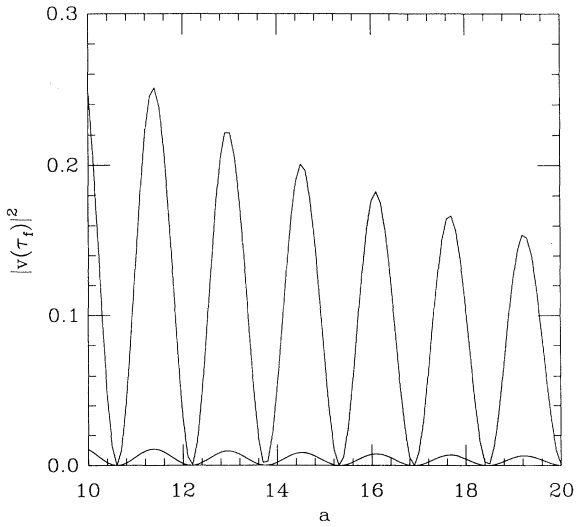

FIG. 11. Plot of the transition probability for Eq. (60) in the sudden limit as a function of a for $b=0.10$. The lower line is the result after one period; the upper line is the result after five periods, and is a simple multiple of the lower line. No resonances due to phase relationships are predicted or observed.

$$\bar{v}(\tau_f)=-ib\int_{\tau_i}^{\tau_f}e^{-2i\kappa t}\left[J_0(a)+2\sum_{n=1}^{\infty}(-1)^nJ_{2n}(a)\cos 2nt+i(-1)^{n-1}J_{2n-1}(a)\cos(2n-1)t\right]dt$$

$$=\lim_{\nu\to 0}-ib\left\{J_0(a)\frac{e^{-2i\kappa\tau}}{-2i\kappa}+\sum_{n=1}^{\infty}\left[(-1)^nJ_{2n}(a)\left[\frac{e^{2i(n-\tilde{\kappa})\tau}}{2i(n+\tilde{\kappa})}+\frac{e^{-2i(n-\tilde{\kappa})\tau}}{-2i(n+\tilde{\kappa})}\right]\right.\right.$$

$$\left.\left.+i(-1)^{n-1}J_{2n+1}(a)\left[\frac{e^{i(2n+1-2\tilde{\kappa})\tau}}{i(2n+1-2\tilde{\kappa})}+\frac{e^{-i(2n+1+2\tilde{\kappa})\tau}}{-i(2n+1+2\tilde{\kappa})}\right]\right]\right\}\Bigg|_{\tau_i}^{\tau_f}, \quad (66)$$

where $\tilde{\kappa}\equiv\kappa+i\nu$ is used to avoid ambiguities regarding divergences, taking $\nu\to 0$ at the end of all calculations.

In Fig. 12 we plot transition probability calculated from Eq. (66), taking the first 40 terms. Direct independent numerical solutions of the differential Eq. (39) yield results that cannot be distinguished from those of Eq. (66), as plotted in the figure. We note that it is substantially different from the unperturbed results of Fig. 11; for different choices of the offset κ, we may dramatically enhance or suppress the transition probability over a single period.

The resonance occurs whenever the phase difference between the diagonal elements of the transition matrix is an integral multiple of π. This requires that

$$\alpha=\left[\frac{1}{2}\right]2(a\cos\tau-\kappa\tau)\Big|_{\tau_i}^{\tau_f}=2\pi\kappa=n\pi\ , \quad (67)$$

or

$$\kappa=n/2\ . \quad (68)$$

This is confirmed by the independent numerical solution of Eq. (63). In Fig. 13 we see that after ten periods, dramatic peaks in the transition probability do indeed appear at the points $\kappa=n/2$. Note that there is *no* hint of such structure in the single period transition probabilities plotted in Fig. 12.

Thus we have illustrated the principle outlined in Sec. III B. Whenever there is no phase difference between the diagonal elements of the time-evolution matrix (that is, whenever $\alpha=n\pi$), we see a resonance in the transition amplitude. This resonance can be extremely sharp.

D. Application of transfer matrix technique to Josephson junctions

Armed with the above understanding of two-state systems, we now approach the Josephson junction case. For the parameters of interest, the two lowest instantaneous eigenstates (Fig. 4) resemble those of the two-level case in the adiabatic limit. Indeed it can be shown that the bottleneck in the junction case is transferring amplitude from the lowest band to the next higher band; all subsequent transitions occur with higher rates.[46] With this in mind, we truncate the infinite dimensional time evolution matrix U_0 and consider only transitions between the lowest two states in the adiabatic limit. The sudden limit

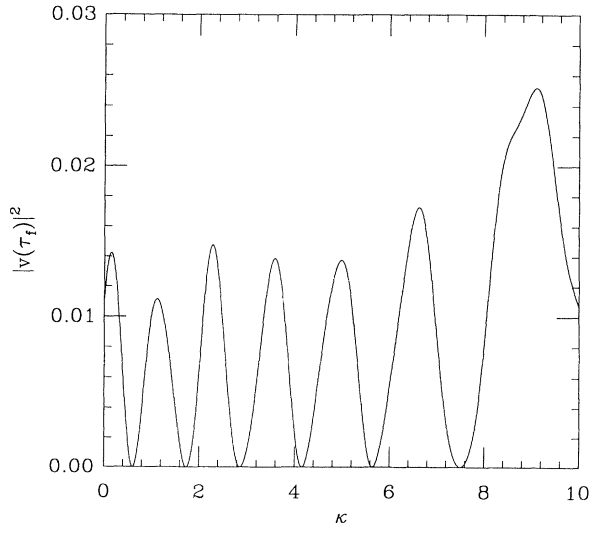

FIG. 12. Plot of the transition probability $|\bar{v}(\tau)|^2$ after a single period, as a function of κ in the sudden limit. The parameters are $a=0.10$ and $b=10.0$. Note that by varying the offset energy κ we may dramatically enhance or suppress the transition probability.

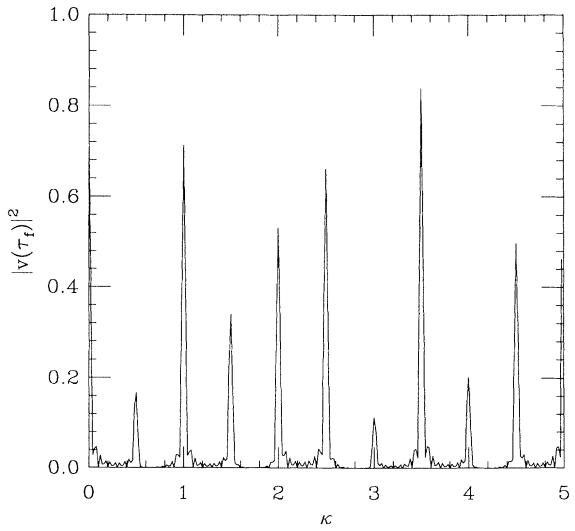

FIG. 13. Plot of the transition probability $|\bar{v}(\tau)|^2$ as in Fig. 12, after ten periods. The peaks occur whenever $\kappa=n/2$, as predicted by Eq. (6). At precisely these values of κ, the phase difference between the diagonal elements of the transfer matrix vanishes.

is not of interest for this particular problem, since the system will then simply Zener tunnel upward without limit.

We calculate the matrix elements of U_0 in the adiabatic limit. As in the two-level case above, we solve for the instantaneous eigenstates which obey

$$i\beta E_n(s)v_n(\theta,s)=\left[\left[-i\frac{\partial}{\partial\theta}-s\right]^2+\lambda(1-\cos\theta)\right]v_n(\theta,s)\ . \tag{69}$$

From these we may construct $\varphi(\theta,s)$

$$\varphi(\theta,s)=\sum_{k=1}^{\infty}c_k(s)v_k(\theta,s)\exp\left[\frac{-i}{\beta}\int^s ds' E_k(s')\right]\ . \tag{70}$$

If $\varphi_i(\theta,s)$ is the solution to Eq. (6) with an initial condition $\varphi_i(\theta,0)=v_i(\theta,0)$, then the truncated time evolution matrix in the adiabatic limit is

$$U_0\approx\begin{bmatrix}\exp\left\{(-i/\beta)\int_0^1 ds E_0(s)\right\} & \Gamma\exp\left\{(-i/\beta)\int_0^1 ds E_1(s)\right\}\\ \Gamma^*\exp\left\{(-i/\beta)\int_0^1 ds E_0(s)\right\} & \exp\left\{(-i/\beta)\int_0^1 ds E_1(s)\right\}\end{bmatrix}, \tag{71}$$

where the transition amplitude Γ is given by

$$\Gamma=\int_0^1 ds\left[v_1^*(\theta,s)\frac{\partial}{\partial s}v_0(\theta,s)\right]\times\exp\left\{\frac{i}{\beta}\int_0^s ds'[E_0(s')-E_1(s')]\right\}\ . \tag{72}$$

An analytical expression for Γ is complicated, and the analysis of Sec. III B above shows it to be unnecessary. The resonance simply arises when the relative phase of the diagonal elements in Eq. (71) is a multiple of π,

$$\alpha=\frac{1}{2\beta}\int_0^{2\pi}ds[E_0(s)-E_1(s)]=n\pi\ , \tag{73}$$

in the limit $\lambda\gg1$ we may calculate the energy spectrum of Eq. (18), using the techniques of the tight-binding approximation. It is simple to show that it is of the form[47]

$$E_0(s)-E_1(s)\approx E_{0,1}+\Delta_{0,1}\cos 2\pi s\ , \tag{74}$$

where $E_{0,1}$ is the energy splitting of the estates in a single well, and $\Delta_{0,1}$ corresponds to the overlap energy. If we integrate Eq. (74) over one period, we obtain the resonance condition

$$E_{0,1}=2\pi n\beta\ . \tag{75}$$

This is precisely the condition required for resonant tunneling in the multiple well (or extended) picture, as in Eq. (21), where here the distance between wells is 2π. Thus in the regime of interest, the two resonances are predicted to occur for the same values of the parameters. This result is not dependent upon the tight-binding approximation. The splitting $E_{0,1}$ of the bound states will always be maximal for $s=0$, so that the energy difference will always be of the form of Eq. (74).

To illustrate this further, we calculate the actual complex matrix elements of the 2×2 time evolution operator by solving for Γ numerically. Such a solution involves integrating over only a *single* period. We then perform the multiplication of Eq. (27) explicitly, for large n or long periods of time. In Fig. 14 we compare the two methods. The elements of the transfer matrix were computed both by numerical solution of Eq. (6) over a single period, and by the adiabatic approximation of Eq. (71). Although the transfer-matrix approach is a crude approximation in that it discards the dynamics of all the higher bands, it does indeed show the presence of the resonance and its

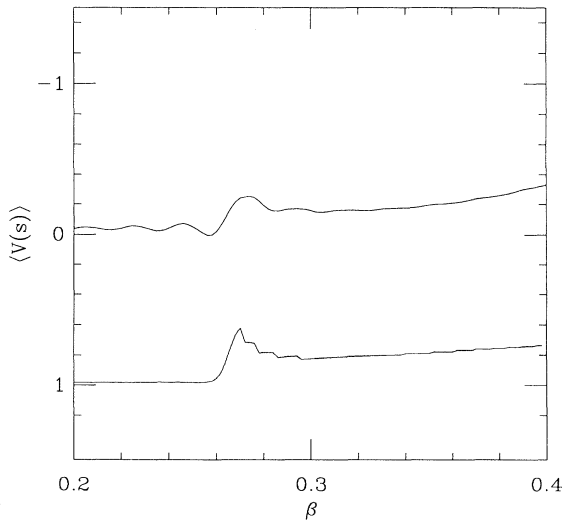

FIG. 14. Comparison of numerical solutions of the time-dependent Schrödinger equation of Eq. (6) (upper curve) and the transfer matrix approach (lower curve). The expectation value of the voltage at $s=It/2e=50$ is calculated in the two approaches, the transfer-matrix result was offset by unity to present it more clearly. Despite the simplicity of the two-band approach, it gives the correct position, magnitude, and approximate shape of the resonance.

qualitative features. Any alteration of the phases of U_0 completely destroys this agreement.

Quantitative predictions of the resonance are also possible. Numerical calculations of the eigenenergies[48] of Eq. (18) give $E_{0,1}=1.757$, so that the resonance is predicted to occur at $E_{0,1}/2\pi=0.279$, in good agreement with the observed position in Fig. 6.

Ao and Rammer have shown that there are similar resonances in superlattices of finite length.[49] Their method is quite similar to the transfer-matrix method used here. Although they do not make the connection between their resonance and the alignment of the energy levels of different wells, they do show that such resonances can be understood within the context of Zener tunneling.

We have now shown that the explanation of the resonances developed in Sec. III B is consistent with the resonance found for Josephson junctions. This explanation, involving the relative phases of the diagonal matrix elements, has been shown to be identical to the resonance condition of the extended problem.

IV. APPLICATIONS TO MESOSCOPIC SYSTEMS

A variety of systems can be described phenomenologically by a Hamiltonian similar to that of Eq. (6), including electrons moving in a superlattice, and Josephson junctions. In Sec. III above, we have shown that an underlying symmetry can lead to resonances in all of these systems, despite the topologically different boundary conditions. What must be present is a discrete time translation symmetry of the time-dependent Schrödinger equation that allows one to relate solutions over a given unit interval.

Moreover, this resonance is not limited to a given regime of parameters. Consider the case of an electron moving in a superlattice. For strong lattice potentials which form a quantum-well structure, we discuss resonant tunneling phenomena; for weak periodic potentials, one instead refers to elastic tunneling between Wannier-Stark states.[35,50,51] The latter requires imposing a Bohr-Sommerfeld quantization condition on closed orbits in k space, a condition identical to our Eq. (56). However, we have seen that this is formally equivalent to the resonant tunneling condition. The fundamental underlying structure is the same.

The principle behind resonant Zener tunneling is merely that the phases between diagonal elements of the time-evolution matrix must be a multiple of π. This can be seen perhaps more clearly in the familiar context of the adiabatic approximation. If we wish to calculate the Zener tunneling rate in the adiabatic limit, then we must, in general, perform an integral of the form

$$A(n\tau_0)=\int_0^{n\tau_0} d\tau\, G(\tau)e^{iF(\tau)}\ , \tag{76}$$

as calculated in Sec. III B. We assume that due to some symmetry of the problem, $G(\tau)$ is periodic in τ_0. If the function $F(\tau)$ is not periodic in τ_0, then contributions from different intervals of the integral will cancel and we will not see any net accumulation. This is equivalent to requiring $\alpha=m\pi$.

There are several advantages to formulating the resonance condition in terms of the transfer matrix. First, the phenomena need not be an adiabatic one, as shown in Sec. III C. Second, it is usually easy to calculate the instantaneous energies, while performing the full integral in the adiabatic approximation is often difficult. Third, it gives us insight into problems like that posed in Sec. II, where we considered the effect of boundary conditions on the current driven Josephson junction. Once it is realized that the resonances are due to a relationship between the elements of the time evolution matrix, it becomes apparent that the boundary conditions are not the relevant issue. Finally, if one wishes to calculate the full time evolution of the problem, the transfer-matrix approach is more stable. Once U_0 is know, the solution at time $n\tau_0$ is easy to obtain. It is possible to obtain accurate values for the elements of the transfer matrix by numerically solving the time-dependent Schrödinger equation over a single period using a fine time step, much finer than would be possible if one were solving the differential equation over the full time interval $n\tau_0$.

This is not to say that *all* resonant or elastic tunneling phenomena should be understood in this context. Many, if not most, externally driven systems do not possess the required symmetry. Nor do we wish to claim that two systems are identical because the two models have similar resonances because of similar symmetries. Indeed, we have shown that the compact and extended formulation of the junction problem can yield different values for observables.

It is important to note that although the two-level system developed in Sec. III C was used as a toy model to study the dynamics of the junction problem, it is an important physical system in its own right. It is directly applicable to experiments in nuclear magnetic resonance and electron-spin relaxation.[52] Very few experiments have been done to directly examine Zener tunneling. It is more commonly used in scattering experiments where it is assumed that the particles follow their classical trajectory [$\mathbf{r}_1(t)$ and $\mathbf{r}_2(t)$], so that the interaction energy $V[\mathbf{r}_1(t)-\mathbf{r}_2(t)]$ is a time-dependent c-number potential. It would be quite useful to have an experimental system which more closely resembles the two-level system described above. NMR and ESR are extremely well characterized, and would be ideal for such measurements. Moreover, there are several theoretical predictions for how environmental degrees of freedom might affect Zener tunneling.[43,44] The coupling between nuclear spins and their environment is understood sufficiently well that it may be possible to make quantitative comparisons between theory and experiment.

We close by considering the relevance of this study to some vexing issues regarding Josephson junctions.

From first principles it seems that the proper way to describe the phase across a Josephson junction is the compact formulation of Eq. (2). We have shown that this is in general not equivalent to the solution of the extended problem of Eq. (1). For damped junctions such as those used in macroscopic tunneling experiments, there may be little differences in the two cases. However, there are regimes where solving the washboard problem will

give incorrect results to Eq. (2).

There are certain other physical situations in which it may be meaningful to consider phase changes by more than 2π. For example, consider the simple Josephson junction in Fig. 15. If the wires which connect the two sides of the junction are also made from superconducting material, then one can imagine following the phase of the order parameter continuously around the loop from one side of the junction to the other. In such a case it seems reasonable to define phase differences that are in excess of 2π. On the other hand, we may insert a small segment of normal metal very far from the junction itself, so that it becomes unclear what physical meaning can be assigned to phase differences larger than 2π. Yet it seems unreasonable that the physics of junction should depend upon the presence or absence of phase coherence at long distances from the junction.

Some researchers have, in effect, tried to circumvent the issue by appealing to dissipation. It is possible to couple the phase coordinate or the charge coordinate to a bath of harmonic oscillators. Zwerger, Dorsey, and Fisher coupled a bath to the momentum coordinate.[26] However, they did so in such a way that the phase symmetry $\psi(\theta)\rightarrow\psi(\theta+2\pi)$ was broken in the initial conditions.[29] Apenko has done something similar, writing down a Hamiltonian for a system driven by continuous charge.[27] It is not entirely clear when continuous charge may be invoked for a mesoscopic system. Apenko then proves decompactification of the phase only for thermodyanmic expectation values, and not for dynamical quantities. However remnants of interference terms can be present in the latter when absent in the former.

It seems most reasonable to calculate the dynamics of a system in which the bath is coupled to $\sin\theta$ and $\cos\theta$. Indeed, that is the way the dissipation mechanisms were originally formulated for Josephson junctions.[53] However, such couplings are as yet analytically intractable. Furthermore, if we Fourier transform such terms as in Eq. (8) or Eq. (10), we find they still only relate coefficients with $\Delta k=\pm 1$ or $\Delta m=\pm N$. This suggests that a bath coupled to $\sin\theta$ and $\cos\theta$ may not decompactify the phase.

Normally one is concerned with the extreme charging or Josephson limits. In this work the regime $\lambda\gtrsim 1$ seems to be peculiar; if we only consider the voltage and its moments, then this is the case where the distinction between the compact and extended cases has a significant time-dependent difference. Trivially, it is in this regime that there exist a small number of bound states in each well of the washboard potential. Perhaps of deeper significance may be that for $\lambda\approx 1$, the charge and phase variables are approximately self-dual. This regime is of particular interest in 2D superconducting films.[54]

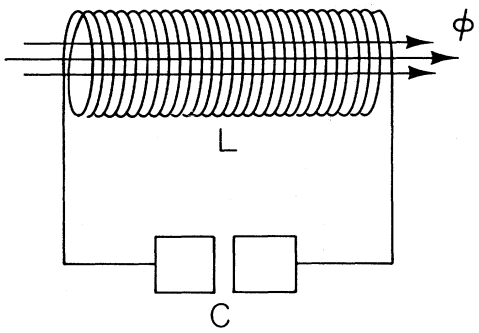

FIG. 15. A schematic representation of a Josephson junction. The junction is driven by a time-dependent external flux, producing a voltage $L\dot{\phi}$ external constant current source. The connecting wires may be superconducting or insulating.

In conclusion, there are several intriguing open questions regarding the quantum dynamics of Josephson junctions. These issues arise only for $E_C\sim E_J$, not the conventional limits where either the charging or Josephson energy dominates. Since this is an experimentally accessible regime, there exist possibilities for observations in the near future.

ACKNOWLEDGMENTS

We thank the MacArthur Foundation for support during this research. One of us (D.L.) also thanks the Swiss National Science Foundation for support, while another (K.M.) was also supported by Grant NSF DMR-9113911 from the National Science Foundation. We are grateful to D. Arovas, K. Burke, S. Girvin, and A. J. Leggett for discussions.

APPENDIX: COMPARISON OF COMPACT AND EXTENDED APPROACHES FOR THE FREE CASE

The free ($\lambda=0$) case is useful to consider since we can solve the time-dependent Schrödinger equation exactly. We wish to show that the compact and extended approaches can yield different results for observables. We rewrite Eq. (6) as

$$i\frac{\partial}{\partial\tau}\psi(\theta,\tau)=\left[-i\frac{\partial}{\partial\theta}-\beta\tau\right]^2\psi(\theta,\tau)\ , \tag{A1}$$

so that we may take the limit $\beta\rightarrow 0$ if desired. We make the further substitution $\theta=N\zeta$, where ζ is the polar angle on the circle of radius N. We now have

$$i\frac{\partial}{\partial\tau}\psi(\zeta,\tau)=\left[-\frac{i}{N}\frac{\partial}{\partial\zeta}-\beta\tau\right]^2\psi(\zeta,\tau)\ . \tag{A2}$$

The solution is easily found by Fourier transforms. We write

$$\psi(\zeta,\tau)=\frac{1}{2\pi}\sum_{k=-\infty}^{\infty}a_k(\tau)e^{ik\zeta}\ . \tag{A3}$$

Inserting this into Eq. (A2), we can obtain

$$i\frac{\partial}{\partial\tau}a_k(\tau)=\left[\frac{k}{N}-\beta\tau\right]^2a_k(\tau)\ , \tag{A4}$$

which has the solution

$$\begin{aligned}a_k(\tau)&=\bar{a}_k e^{(i/3\beta)(k/N-\beta\tau)^3}\\&=\bar{a}_k e^{i[(k^2/N^2)\tau+(k/N)\beta\tau^2+i(\beta^3/3)\tau^3]}\ ,\end{aligned} \tag{A5}$$

where we have absorbed a factor of $e^{ik^3/3\beta N^3}$ into the con-

stant $\tilde{a}_k$.

From this we see that we need only Fourier transform the initial conditions and we have a solution for all times. This can also be understood by noting that $[H,\hat{n}]=0$, so that each component is unchanged in time.

As an initial condition for the extended case we choose

$$\psi_e(\xi_0)=\begin{cases}\dfrac{1}{\sqrt{2\pi}} & \text{for } \xi<2\pi/N\ ,\\ 0 & \text{otherwise}\ .\end{cases} \tag{A6}$$

If we express this in terms of the Fourier expansion, we obtain

$$\tilde{a}_k=\begin{cases}\dfrac{e^{-2\pi ik/N}-1}{-i\sqrt{2\pi}k} & \text{for } k\neq 0\ ,\\ \sqrt{2\pi}N & \text{for } k=0\ ,\end{cases} \tag{A7}$$

so that

$$\psi_e(\xi,\tau)=\frac{1}{\sqrt{2\pi}N}+\frac{i}{(2\pi)^{3/2}}\times\sum_k{}'\frac{e^{-2\pi ik/N}-1}{k}\times e^{ik\xi}e^{i[(k^2/N^2)\tau+(k/N)\beta\tau^2+i(\beta^3/3)\tau^3]}\ , \tag{A8}$$

where the prime on the sum indicates that the $k=0$ term is omitted. For the compact case, we simply repeat $\psi(\xi,0)$ around the ring and then normalize; this produces an initial condition: $\psi_c(\xi,0)=1/\sqrt{2\pi N}$ which gives the solution

$$\psi_c(\xi,\tau)=\frac{1}{\sqrt{2\pi N}}e^{i(\beta^3/3)\tau^3}\ . \tag{A9}$$

We can calculate $\langle n\rangle$ and $\langle n^2\rangle$ for the two cases; we may ignore the time dependence since both commute with the Hamiltonians. In the compact case, since the wave function is a constant, we see

$$\begin{aligned}\langle n\rangle_c&=0\ ,\\ \langle n^2\rangle_c&=0\ .\end{aligned} \tag{A10}$$

For the extended case.

$$\begin{aligned}\langle n\rangle_e&=\frac{1}{(2\pi)^3}\sum_k{}'\frac{|e^{-2\pi ik/N}-1|^2}{Nk}\\ &=\frac{1}{(2\pi)^3}\sum_k{}'\frac{\sin^2\pi k/N}{Nk}=0\ ,\\ \langle n^2\rangle_e&=\frac{1}{(2\pi)^3}\sum_k{}'\frac{\sin^2\pi k/N}{N^2}=\infty\ ,\end{aligned} \tag{A11}$$

where $\langle n^2\rangle_e$ diverges from fixed N. The order of limits is important; the sum is calculated for fixed N, and then N is taken to ∞, which yields a divergent result. This result is truly independent of λ at $\tau=0$; it is true for all times in the free case.

The key difference between the two cases is that "chopping" the wave function so that it fits exactly into one well introduces discontinuities in ψ and/or its derivatives. If we choose a function that is not discontinuous on the boundaries, such as $\sin N\xi$ or $\sin^2 N\xi$, these discontinuities appear in the higher moments of $\hat{n}$. (It is not possible for an analytic function to be nonzero at any point and then zero over a continuous interval.) They will therefore show up in the equation of motion of the operators whenever $\hat{n}$ or $\sin\hat{\theta}$ cannot be approximated well by their expectation values. This will happen when $\lambda\approx 1$, which is consistent with the understanding developed in the text. Alternatively, one can think of the chopping as introducing many modes in Fourier space which are not multiples of N, and thus not representable in the compact problem.

It is curious to note that in the free case, the δ function's initial conditions yield the same dynamics for the two models. The Fourier transforms of the extended and compact initial conditions are both periodic arrays of δ functions with identical moments.

*Permanent address.

[1]M. Büttiker, Y. Imry, and R. Landauer, Phys. Lett. **96A**, 365 (1983).

[2]R. Landauer and M. Büttiker, Phys. Rev. Lett. **54**, 2049 (1985).

[3]Y. Meir, Y. Gefen, and O. Entin-Wohlman, Phys. Rev. Lett. **63**, 798 (1989).

[4]D. Loss, P. Goldbart, and A. Balatsky, Phys. Rev. Lett. **65**, 1665 (1990).

[5]A. J. Leggett, in *Proceedings of the NATO Advanced Study Institute on Granular Nano-electronics,* edited by D. K. Ferry (Il Ciocco, Italy, 1990).

[6]D. Loss and P. Goldbart, Phys. Rev. B **45**, 13 544 (1992).

[7]R. Landauer, IBM Jr. Res. Ref. **1**, 2203 (1957).

[8]R. Landauer, Philos Mag. **21**, 683 (1970).

[9]For a review of conductance formulas, see M. Büttiker in *Electronic Properties of Multilayers and Low Dimensional Semiconductor Devices,* edited by J. M. Chamberlain and J. C. Portal (Plenum, New York, in press).

[10]Y. Imry, in *Directions in Condensed Matter Physics,* edited by G. Grinstein and G. Mazenko (World Scientific, Singapore, 1986).

[11]B. D. Josephson, Phys. Lett. **1**, 251 (1962).

[12]A. J. Leggett, Prog. Theor. Phys. Suppl. **69**, 80 (1980).

[13]M. Martinis, M. H. Devoret, and J. Clarke, Phys. Rev. B **35**, 4682 (1987).

[14]V. Voss and R. A. Webb, Phys. Rev. Lett. **47**, 265 (1981).

[15]S. Washburn, R. A. Webb, R. F. Voss, and S. F. Faris, Phys. Rev. Lett. **54**, 2712 (1985).

[16]D. Esteve, J. M. Mirinis, C. Urbina, E. Turlot, and M. H. Devoret, Phys. Scr. **T29**, 121 (1989).

[17]E. Ben-Jacob and Y. Gefen, Phys. Lett. A **108**, 289 (1985).

[18]A. I. Larkin, K. K. Likharev, and Yr. N. Ouchinnikov, Physica **126B+C**, 414 (1984).

[19]M. Büttiker, Phys. Scr. **T14**, 12 (1986).

[20]M. Büttiker, Phys. Rev. B **36**, 3548 (1987).

[21]T. A. Fulton and G. J. Dolan, Phys. Rev. Lett. **59**, 109 (1987).

[22]J. B. Barner and S. T. Ruggiero, Phys. Rev. Lett. **59**, 807 (1987).

[23]L. S. Kuz'min and K. K. Likharev, Pis'ma Zh. Eksp. Teor. Fiz. **45**, 306 (1987) [JETP Lett. **45**, 387 (1987)].

[24]R. Wilkins, E. Ben-Jacob, and R. Jaklevic, Phys. Rev. Lett. **63**, 801 (1989).
[25]K. K. Likharev and A. B. Zorin, J. Low Temp. Phys. **59**, 347 (1985).
[26]W. Zwerger, A. Doresey, and M. P. A Fisher, Phys. Rev. B **34**, 6518 (1986).
[27]K. K. Likharev, in *Mesoscopic Phenomena in Solids,* edited by B. L. Altshuler, P. A. Lee, and R. Webb (Elsevier, New York, 1991).
[28]D. Loss and K. Mullen, Phys. Rev. A **43**, 2129 (1991).
[29]A. Davidson and P. Santhanam, Phys. Lett. A **149**, 476 (1990).
[30]S. M. Apenko, Phys. Lett. A **142**, 277 (1989).
[31]N. Hatakenaka, S. Kurihara, and H. Takayanagi, Phys. Rev. B **42**, 3987 (1990).
[32]J. M. Schmidt, A. N. Cleland, and J. Clarke, Phys. Rev. B **43**, 229 (1991).
[33]P. Carruthers and M. M. Nieto, Rev. Mod. Phys. **40**, 411 (1968).
[34]D. Loss and K. Mullen, J. Phys. A **25**, L235 (1992).
[35]J. B. Krieger and G. J. Iafrate, Phys. Rev. B **33**, 5494 (1986).
[36]To be more precise, in writing down the Fourier expansion of Eq. (7), we have implicitly extended the function in a periodic fashion, for the right-hand side is defined for arbitrary values of θ. Similarly, we have done the same in Eq. (9), but with a period $2\pi N$. Neither of these two procedures should be confused with the construction of ψ_c, which requires a periodic repetition and rescaling of the original function.
[37]N. W. McLachlan, *Theory and Application of Mathieu Functions* (Clarendon, Oxford, 1947), p. 19.
[38]G. D. Smith, *Numerical Solution of Partial Differential Equations: Finite Difference Methods* (Clarendon, Oxford, 1985).
[39]C. Zener, Proc. R. Soc. London, Ser. A **137**, 696 (1932).
[40]L. Landau, Sov. Phys. **1**, 89 (1932); Z. Phys. Sov. **2**, 1932 (1932).
[41]S. Fishman, K. Mullen, and E. Ben-Jacob, Phys. Rev. A **42**, 5181 (1990).
[42]I. Goldhirsh, D. Lubin, and Y. Gefen, Phys. Rev. Lett. **67**, 3582 (1991).
[43]P. Ao and J. Rammer, Phys. Rev. B **43**, 5395 (1991).
[44]E. Shimshoni and Y. Gefen, Ann. Phys. (NY) **210**, 10 (1991).
[45]S. K. Ma, *Statistical Mechanics* (World Scientific, Philadelphia, 1985).
[46]E. Ben-Jacob, Y. Gefen, K. Mullen, and Z. Schuss, Phys. Rev. B **37**, 7400 (1988).
[47]J. M. Ziman, *Principles of the Theory of Solids* (Cambridge University Press, Cambridge, England, 1964).
[48]For $\lambda \gg 1$ the lowest eigeneneriges of Eq. (18) can be approximated as harmonic oscillator states. However, when there are few bound states, the eigenenergies must be calculated numerically.
[49]P. Ao and J. RAmmer, Phys. Rev. B **44**, 11 494 (1991).
[50]G. H. Wannier, Phys. Rev. **117**, 432 (1960).
[51]G. H. Wannier and D. R. Fredkin, Phys. Rev. **125**, 1910 (1962).
[52]C. P. Slichter, *Principles of Magnetic Resonance* (Springer-Verlag, New York, 1980).
[53]U. Eckern, G. Schön, and V Ambegaokar, Phys. Rev. B **30**, 6419 (1984).
[54]S. Girvin (private communication).